

AD-A058 141

ARNOLD ENGINEERING DEVELOPMENT CENTER ARNOLD AIR FORC--ETC F/G 22/2
TEST RESULTS FROM THE NASA/ROCKWELL INTERNATIONAL SPACE SHUTTLE--ETC(U)
JUN 78 K W NUTT

UNCLASSIFIED

AEDC-TSR-78-V15

NL

1 OF 1
ADA
058141



END
DATE
FILMED
10-78
DDC

ADA 058141

AEDC-TSR-78-V15
JUNE 1978

B029096

(2)

TEST RESULTS FROM THE NASA/ROCKWELL INTERNATIONAL
SPACE SHUTTLE INTEGRATED VEHICLE TEST (IH 85)
CONDUCTED IN THE AEDC-VKF TUNNEL A



Kenneth W. Nutt
ARO, Inc., AEDC Division
A Sverdrup Corporation Company
von Kármán Gas Dynamics Facility
Arnold Air Force Station, Tennessee

LEVEL *111*

Period Covered: April 19-26, 1978

APPROVED FOR PUBLIC RELEASE; DISTRIBUTION UNLIMITED.

AU NO.

DDC FILE COPY

Reviewed by:

Ervin P. Jaskolski

ERVIN P. JASKOLSKI, Capt, USAF
Test Director, VKF Division
Directorate of Test Operations

Approved for Publication:
FOR THE COMMANDER

Chauncey D. Smith, Jr.
CHAUNCEY D. SMITH, JR, Lt Colonel, USAF
Director of Test Operations
Deputy for Operations

Prepared for: Johnson Space Center
(NASA-JSC)(ES3)
Houston, TX

DDC
RECEIVED
AUG 29 1978
REGISTERED

78 08 28 127
ARNOLD ENGINEERING DEVELOPMENT CENTER
AIR FORCE SYSTEMS COMMAND
ARNOLD AIR FORCE STATION, TENNESSEE

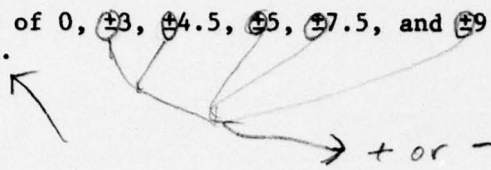
UNCLASSIFIED

REPORT DOCUMENTATION PAGE		READ INSTRUCTIONS BEFORE COMPLETING FORM
1. REPORT NUMBER 14 AEDC-TSR-78-V15	2. GOVT ACCESSION NO.	3. RECIPIENT'S CATALOG NUMBER 9
4. TITLE (and Subtitle) 6 Test Results from the NASA/Rockwell International Space Shuttle Integrated Vehicle Test (IH 85) Conducted in the AEDC-VKF Tunnel A,		5. TYPE OF REPORT & PERIOD COVERED Final Report, April 1978 April 20, 1978
		6. PERFORMING ORG. REPORT NUMBER
7. AUTHOR(s) 10 Kenneth W. Nutt ARO, Inc., a Sverdrup Corporation Company		8. CONTRACT OR GRANT NUMBER(s)
9. PERFORMING ORGANIZATION NAME AND ADDRESS Arnold Engineering Development Center Air Force Systems Command Arnold Air Force Station, TN 37389		10. PROGRAM ELEMENT, PROJECT, TASK AREA & WORK UNIT NUMBERS Program Element 921E-01 17 622d2F
11. CONTROLLING OFFICE NAME AND ADDRESS Johnson Space Center (NASA-JSC) (ES3) Houston, TX 11		12. REPORT DATE June 1978
14. MONITORING AGENCY NAME & ADDRESS (if different from Controlling Office)		13. NUMBER OF PAGES 41 (1244p)
		15. SECURITY CLASS. (of this report) Unclassified
		15a. DECLASSIFICATION DOWNGRADING SCHEDULE N/A
16. DISTRIBUTION STATEMENT (of this Report) Approved for public release; distribution unlimited.		
17. DISTRIBUTION STATEMENT (of the abstract entered in Block 20, if different from Report)		
18. SUPPLEMENTARY NOTES Available in DDC		
19. KEY WORDS (Continue on reverse side if necessary and identify by block number) Heat Transfer Space Shuttle Supersonic Testing Interference Heating		
20. ABSTRACT (Continue on reverse side if necessary and identify by block number) Tests were conducted in the AEDC-VKF Supersonic Wind Tunnel A to obtain convective heat-transfer-rate distributions on the Space Shuttle Integrated Vehicle during simulated first and second stage conditions of the flight profile. The test model was a 0.0175-scale model (60-OTS), of the Rockwell International Vehicle 5 configuration. Model configurations tested included the Integrated Vehicle and the Orbiter/External Tank with the Solid Rocket Boosters removed. The tests were conducted at Mach numbers 3 and 4 using the thin-skin thermocouple technique. The model was tested at angles of attack of 0, 2.5, and		

78 08 28
for -
127
Dme

UNCLASSIFIED

± 5 deg and at yaw angles of 0, ± 3 , ± 4.5 , ± 5 , ± 7.5 , and ± 9 deg. A test description is presented.



ACCESSIBLE BY	
TYPE	Other Services <input checked="" type="checkbox"/>
SEC	Ref. Control <input type="checkbox"/>
DISSEMINATED	<input type="checkbox"/>
RESTRICTED	<input type="checkbox"/>
DISTRIBUTION/AVAILABILITY CODE	
Doc	AVAIL. cont. or OTHER
A	

AFSC
Arnold AFB Tex

UNCLASSIFIED

CONTENTS

	<u>Page</u>
NOMENCLATURE	2
1.0 INTRODUCTION	6
2.0 APPARATUS	
2.1 Test Facility	6
2.2 Test Article	7
2.3 Test Instrumentation	
2.3.1 Test Conditions	7
2.3.2 Test Data	8
3.0 TEST DESCRIPTION	
3.1 Test Conditions	8
3.2 Test Procedure	
3.2.1 General	8
3.2.2 Data Acquisition	9
3.2.3 Data Reduction	9
3.3 Adiabatic Wall Temperature	11
3.4 Uncertainty of Measurements	
3.4.1 Test Conditions	13
3.4.2 Test Data	14
4.0 DATA PACKAGE PRESENTATION	14
REFERENCES	15

APPENDIXES

A. ILLUSTRATIONS

Figure

1. Tunnel A	17
2. Sketch of the Space Shuttle Integrated Model	18
3. External Tank Nose Tip Configuration	19
4. Model Installation in Tunnel A	20
5. Typical Heat-Transfer Data Tabulation	21
6. Comparison of External Tank Data for the OTS Configuration with Theory and Results from a Previous Test at Mach 3.01	22
7. Comparison of External Tank Data for the OTS Config- uration with Theory and Results from a Previous Test at Mach 4.02	23

B. TABLES

Table

1. Thermocouple Constant Sets	25
2. Test Data Summary	37
3. Equations for Calculating Local Surface Angle of Attack on the Orbiter Model	41

NOMENCLATURE

a_1, a_2, a_3	Denote constant terms used to calculate R
ALPHA-MODEL, α_m	Model angle of attack, deg
ALPHA-PREBEND	Sting prebend, deg
ALPHA-SECTOR, α_s	Tunnel sector angle, deg
b	Model wall thickness, ft
CONSTANT SET	Identification of thermocouple hookup (see Table 1)
c_p	Model wall specific heat, $\frac{\text{Btu}}{\text{lbm} \cdot ^\circ\text{R}}$
C.R.	Center of rotation
DELTABF, DABF	Body flap deflection angle, deg
DELTAE, DAE	Elevon deflection angle, deg
DELTASB, DASB	Speed brake deflection angle, deg
DTWDT, dTW/dt	Derivative of the model wall temperature with respect to time, $^\circ\text{R}/\text{sec}$
FS	Full scale
GROUP	Identification number for each tunnel injection
H(TAW)	Heat-transfer coefficient, $\frac{\text{QDOT}}{\text{TAW} - \text{TW}}, \frac{\text{Btu}}{\text{ft}^2 \cdot \text{sec} \cdot ^\circ\text{R}}$
H(TO)	Heat-transfer coefficient, $\frac{\text{QDOT}}{\text{TO} - \text{TW}}, \frac{\text{Btu}}{\text{ft}^2 \cdot \text{sec} \cdot ^\circ\text{R}}$
H(0.95TO)	Heat-transfer coefficient, $\frac{\text{QDOT}}{(0.95\text{TO}) - \text{TW}}, \frac{\text{Btu}}{\text{ft}^2 \cdot \text{sec} \cdot ^\circ\text{R}}$
H(RTO)	Heat-transfer coefficient, $\frac{\text{QDOT}}{(\text{RTO}) - \text{TW}}, \frac{\text{Btu}}{\text{ft}^2 \cdot \text{sec} \cdot ^\circ\text{R}}$

HREF, HREF-FR	Reference heat-transfer coefficient based on Fay-Riddell theory, $\text{Btu/ft}^2\text{-sec-}^\circ\text{R}$
	$\text{HREF} = \frac{8.17173(\text{PO1})^{0.5}(\text{MU-0})^{0.4}[1 - (\text{P-INF}/\text{PO1})]^{0.25}}{(\text{RN})^{0.5}(\text{TO})^{0.15}}$
	x [0.2235 + 0.0000135 [TO + 560]]
L	Axial reference length, in. (see Fig. 2)
M_e	Mach number at boundary layer edge
MACH NO., M_∞	Free stream Mach number
MODEL	Model configuration
MU-0	Viscosity conditions based on stagnation temperature, lb-sec/ft^2
MU-INF	Free-stream viscosity, lb-sec/ft^2
OTS	Orbiter, external tank, and both solid rocket boosters
OT	Orbiter and external tank
P-INF, p_∞	Free-stream pressure, psia
PO, p_o	Tunnel stilling chamber pressure, psia
PO1	Stagnation pressure downstream of a normal shock, psia
QDOT	Heat-transfer rate, wbc_p (DTWDT), $\text{Btu/ft}^2\text{-sec}$
Q-INF, q_∞	Free-stream dynamic pressure, psia
r	Recovery factor
R	Radius or analytical temperature ratio, TAW/TO
RN	Reference nose radius, (0.0175 ft)
RE/FT	Free-stream Reynolds number per foot, ft^{-1}
RHO-INF	Free-stream density, lbm/ft^3
ROLL-MODEL	Model roll angle, deg

SRB Solid Rocket Booster

STFR Theoretical stagnation point Stanton number for a 0.0175-ft (1 scale foot) radius sphere calculated from Fay-Riddell theory

$$STFR = \frac{HREF}{(\rho_{\infty} - \rho_{\infty}) (V_{\infty} - V_{\infty}) [0.2235 + 0.0000135(T_0 + 560)] (32.174)}$$

SWITCH POSITION Designates the position of the thermocouple selector switch

t Time from start of model injection cycle, sec

T Temperature, °R

TAW Adiabatic wall temperature, °R

TC-NO, T/C Thermocouple

T-INF Free-stream temperature, °R

T₀, T_o Tunnel stilling chamber temperature, °R

TW Model wall temperature, °R

V-INF Free-stream velocity, ft/sec

w Model wall density, lbm/ft³

X Axial coordinate, in. (see Fig. 2)

Y₀ Orbiter lateral coordinate, in. (see Fig. 2)

X/L Thermocouple axial location as a ratio of model length from model nose tip

YAW Model yaw angle, deg

β Angle of sideslip, equal to negative yaw angle, deg

γ Ratio of specific heat

δ Local surface angle of attack, deg

ε Combination of model roll angle and θ or ψ, deg

θ, THETA External tank angular measurement, deg

λ	Local model deflection angle, deg
ϕ , PHI	Orbiter angular measurement, deg
ψ , PSI	Solid rocket booster angular measurement, deg

Subscripts

e	Flow properties at boundary layer edge
i	Initial conditions
O	Orbiter
S	Solid Rocket Booster
T	External tank
∞	Free-stream flow properties

1.0 INTRODUCTION

The work reported herein was conducted at the Arnold Engineering Development Center (AEDC), Air Force Systems Command (AFSC), by ARO, Inc., AEDC Division (a Sverdrup Corporation Company), contract operator of AEDC, AFSC, Arnold Air Force Station, Tennessee. The work was sponsored by the Johnson Space Center (NASA-JSC(ES3)), Houston, Texas, under Program Element 921E-01. Rockwell International (RI), Space Division, Downey, California was responsible for test planning and data analysis. The project monitor for NASA-JSC(ES3) was Mrs. Dorothy B. Lee and the test engineer for Rockwell International was Mr. Jim Cummings.

The test was conducted in the 40-in. Supersonic Wind Tunnel (A) at the von Karman Gas Dynamics Facility (VKF) during the period April 19-26, 1978, under ARO Project Number V41A-W5. Data were recorded at Mach numbers 3 and 4 at free stream unit Reynolds numbers of 3.7×10^6 and 4.1×10^6 per foot, respectively. The model angle of attack varied from -5 to 5 deg with model yaw angles varying from -9 to 9 deg. Two model configurations; the OTS configuration composed of the fully integrated model with the orbiter, external tank (ET) and both solid rocket boosters (SRB), and the OT Configuration consisting of the orbiter and the external tank, were tested.

The objective of the test was to obtain updated supersonic heat-transfer rate distributions on the Space Shuttle Vehicle configuration VC72-000002F during simulated first and second stage conditions. Data were recorded from instrumentation on the orbiter, external tank and both solid rocket boosters.

Copies of all the detailed test logs have been transmitted to Rockwell International. Three copies of the final tabulated data are being transmitted with this report to Rockwell International. A data tape will be transmitted to Chrysler Corporation Space Division for their analysis under the Dataman contract. Inquiries to obtain copies of the test data should be directed to NASA-JSC(ES3), Houston, Texas 77058. A microfilm record has been retained in the VKF at AEDC.

2.0 APPARATUS

2.1 TEST FACILITY

Tunnel A is a continuous, closed-circuit, variable density wind tunnel with an automatically driven flexible-plate-type nozzle and a 40-by 40-in. test section. The tunnel can be operated at Mach numbers from 1.5 to 6 at maximum stagnation pressures from 29 to 200 psia, respectively, and stagnation temperatures up to 750°R ($M_\infty = 6$). Minimum operating pressures range from about one-tenth to one-twentieth of the maximum at each Mach number. The tunnel is equipped with a model injection system which allows removal of the model from the test section while the tunnel remains in operation. A description of the tunnel and airflow calibration information may be found in Ref. 1. A schematic view of Tunnel A and the model injection system is shown in Fig. 1, Appendix A.

2.2 TEST ARTICLE

The 60-OTS model is a 0.0175-scale thin-skin thermocouple model of the Rockwell International Vehicle 5 configuration. The model was supplied by Rockwell International. A sketch of the Space Shuttle Integrated model is shown in Fig. 2. The model was constructed of 17-4 PH stainless steel with a nominal skin thickness of 0.030 in. at the instrumented areas. All thermocouples were spot-welded to the thin skin inner surface.

Data were obtained for the orbiter, external tank, and both the right and left SRB (as viewed by the pilot). Two model configurations were investigated during this test. The fully integrated model with the orbiter, external tank, and both the right and left SRB was designated the OTS configuration. The OT configuration consisted of only the orbiter and external tank combination with the forward and aft SRB attachments installed on the external tank. The model configurations are listed under the model headings in the tabulated data.

The spike nose tip (10-deg sharp cone) was installed on the external tank, Fig. 3. The external tank reference length of 32.295 in. in model scale is based on the tank length with the nipple nose attached. This reference length was retained for consistent values of X/L.

The inboard elevons on the orbiter were deflected down 10-deg throughout the test. The orbiter speedbrakes and body flap were set at zero deflection.

Boundary layer trips were used on the orbiter and on each SRB to generate a turbulent boundary layer. The trips consisted of 0.020-in.-diam balls spaced on 0.060-in. centers around a form fitted steel strip. The trips were located at an X/L of 0.04 on the orbiter nose and 0.19 on the nose of each SRB. The nose shape on the external tank effectively tripped the boundary layer.

The installation of the OTS configuration in Tunnel A is illustrated in Fig. 4.

2.3 TEST INSTRUMENTATION

2.3.1 Test Conditions

Tunnel A stilling chamber pressure is measured with a 15-, 60-, 150-, or a 300-psid transducer referenced to a near vacuum. Based on periodic comparisons with secondary standards, the accuracy (a bandwidth which includes 95 percent of the residuals, i.e. 2σ deviation) of these transducers is estimated to be within ± 0.2 percent of reading or ± 0.015 psi, whichever is greater. Stilling chamber temperature is measured with a copper-constantan thermocouple with an accuracy of $\pm 3^\circ\text{F}$ based on repeat calibrations (2σ deviation).

2.3.2 Test Data

The model temperatures were measured with iron-constantan thermocouples with an estimated uncertainty of ± 0.5 percent. Data from over 1000 thermocouples were recorded during the test. A Beckman® 210 analog-to-digital converter was used in conjunction with a Digital Equipment Corp.® (DEC) PDP-11 Computer and a DEC-10 Computer to record the temperature data.

Data from a maximum of 97 thermocouples can be recorded during each tunnel injection. Twelve sets of thermocouples were required to accommodate the large number of thermocouples on this test. These sets are called Constant Sets in the tabulated data. A list of the twelve Constant Sets is given in Table I. This list includes all of the thermocouples that were installed for the test. Several of the listed thermocouples were determined to be inoperative and these have been omitted from the tabulated data. A total of three Constant Sets could be connected at one time. A three position selector switch was used to select the desired Constant Set for each injection. A new series of three Constant Sets could be readily connected using quick disconnect thermocouple plugs with 15 thermocouples per plug.

The dimensional locations of the thermocouples at each position are given in Table I. The angular reference system for the thermocouples is shown in Fig. 2. It is important to note that the top centerline of the external tank and both SRB's is the 0-deg location. This agrees with the reference system used in the IH-72 test. The bottom centerline was used as the 0-deg position on the IH-41, IH-41A, and IH-41B tests.

3.0 TEST DESCRIPTION

3.1 TEST CONDITIONS

The test was conducted at the following nominal conditions:

<u>MACH NO.</u>	<u>PO, psia</u>	<u>TO, °R</u>	<u>HREF, sec-ft²-°R</u>	<u>RE/FT</u>
3.01	37	720	0.055	3.8×10^6
4.02	70	720	0.050	4.1×10^6

Data were obtained at angles of attack of 0, ± 2.5 , and ± 5 deg and at yaw angles ($-\beta$) of 0, ± 3 , ± 4.5 , ± 5 , ± 7.5 , and ± 9 deg.

A test data summary showing all configurations tested and the variables for each is presented in Table 2.

3.2 TEST PROCEDURE

3.2.1 General

In the VKF continuous flow wind tunnels (A, B, C), the model is mounted on a sting support mechanism in an installation tank directly underneath the

tunnel test section. The tank is separated from the tunnel by a pair of fairing doors and a safety door. When closed, the fairing doors, except for a slot for the pitch sector, cover the opening to the tank and the safety door seals the tunnel from the tank area. After the model is prepared for a data run, the personnel access door to the installation tank is closed, the tank is vented to the tunnel flow, the safety and fairing doors are opened, and the model is injected into the airstream. After the data are recorded, the model is retracted into the tank and the sequence is reversed with the tank being vented to atmosphere to allow access to the model in preparation for the next run.

3.2.2 Data Acquisiton

The initial step prior to recording the test data was to cool the model uniformly to approximately 60°F with cooled high pressure air. This was accomplished by providing chilled air from a vortex generator (Hilsch vortex tube, Ref. 2) to a retractable cooling manifold. With the model attitude set at zero pitch the cooling manifold was positioned around the model. Once the cooling cycle was complete the cooling manifold was retracted and the model attitude was established prior to tunnel injection. The model was then injected into the tunnel. When the model reached tunnel centerline, the model was immediately translated forward to clear an area of tunnel induced shock impingement. The thermocouple outputs were scanned approximately 15 times per second starting prior to model injection into the airstream and continuing about 5 seconds after the model reached centerline. After each injection, the cooling cycle was repeated to cool the model to an isothermal state.

3.2.3 Data Reduction

The reduction of thin-skin thermocouple data normally involves only the calorimetric heat balance which in coefficient form is:

$$H(TAW) = wbc_p \frac{dTW/dt}{TAW-TW} \quad (1)$$

For this test a value of 0.95 TO was selected for TAW and equation (1) can be written

$$H(0.95TO) = wbc_p \frac{dTW/dt}{0.95TO-TW} \quad (2)$$

Radiation and conduction losses are neglected in this heat balance and data reduction simply requires evaluation of dTW/dt from the temperature-time data and determination of model material properties. For the present tests, radiation effects were negligible; however, conduction effects can be significant in several regions of the models. To permit identification of these regions and to improve evaluation of the data, the following procedure was used.

Separation of variables and integration of Equation (2) assuming constant w , b , c_p , and T_0 yields

$$\frac{H(0.95T_0)}{wbc_p} (t - t_1) = \ln \left[\frac{0.95T_0 - TW_1}{0.95T_0 - TW} \right] \quad (3)$$

Differentiation of Eq. (3) with respect to time gives

$$\frac{H(0.95T_0)}{wbc_p} = \frac{d}{dt} \ln \left[\frac{0.95T_0 - TW_1}{0.95T_0 - TW} \right] \quad (4)$$

Since the left side of Eq. (4) is a constant, plotting $\ln \left[\frac{0.95T_0 - TW_1}{0.95T_0 - TW} \right]$ versus time will give a straight line if conduction is negligible. Thus, deviation from a straight line can be interpreted as conduction effects.

The data were evaluated in this manner, and generally a linear portion of the curve was used for all thermocouples. A linear least-square curve fit of $\ln [(0.95T_0 - TW_1)/(0.95T_0 - TW)]$ versus time was applied to the data. The data reduction time was delayed for all thermocouples that were influenced by the tunnel induced shock until they had cleared this region. The thermocouples on the external tank and both SRB's with an X/L greater than 0.9 were reduced starting 3.9 seconds after centerline. The thermocouples with an X/L greater than 0.2 on the external tank and an X/L greater than 0.113 on each SRB but not exceeding an X/L of 0.9 were reduced starting at 2.6 seconds after centerline. The remaining thermocouples on the external tank and each SRB were reduced starting at centerline. The thermocouples on the orbiter with an X/L greater than 0.055 were reduced starting at 2.6 seconds after centerline. All other thermocouples on the orbiter were reduced starting at centerline. The curve fit extended for a time span which was a function of the heating rate, as shown on the following list.

<u>Range</u>	<u>No. of Points (Fit Length)</u>
$\frac{dT_W}{dt} > 32$	5
$16 < \frac{dT_W}{dt} \leq 32$	7
$8 < \frac{dT_W}{dt} \leq 16$	9
$4 < \frac{dT_W}{dt} \leq 8$	13
$2 < \frac{dT_W}{dt} \leq 4$	17
$1 < \frac{dT_W}{dt} \leq 2$	25
$\frac{dT_W}{dt} \leq 1$	41

The above time spans were adequate to keep the evaluation of the right side of Eq. (4) within the linear region. The linearity of the fit was substantiated by visual inspection of the cases in question. This visual check of the data was done on the VKF graphics terminal. Strictly speaking, the value of c_p for the material was not constant, and the following relation

$$c_p = 0.0797 + (5.556 \times 10^{-5}) TW, \text{ (17-4 PH stainless steel) Btu/lbm}^\circ\text{R (5)}$$

was used with the value of TW at the midpoint of the curve fit. The maximum variation of c_p over any curve fit was less than 1.2 percent. The value of density used for 17-4 PH stainless steel was

$$w = 490.0 \text{ lbm/ft}^3$$

3.3 ADIABATIC WALL TEMPERATURE

The maximum available tunnel stagnation temperature for each Mach number tested is listed in Section 3.1. With these relatively low stagnation temperatures, the difference between the model wall temperature and recovery temperature was generally small in regions of peak heating. This small temperature difference causes the calculation of the heat-transfer coefficient to be very sensitive to deviations from the actual adiabatic wall temperature. Two values of the heat-transfer coefficient have been calculated based on an assumed constant recovery temperature, namely $H(T_0)$ and $H(0.95T_0)$. To account for changes in the recovery temperature a third value of the heat-transfer coefficient has been tabulated based on an analytical temperature ratio, $R = T_{AW}/T_0$.

The analytical method for determining R was developed by Rockwell International and has been used to calculate $H(RT_0)$. In this method, the following relationships were assumed:

$$R = \frac{T_{AW}}{T_0} \quad (6)$$

and

$$T_{AW} = T_e \left(1 + \frac{\gamma-1}{2} r M_e^2 \right) \quad (7)$$

$$r = 0.898 \text{ for turbulent flow}$$

with r being the recovery factor and the subscript e identifying local properties at the boundary-layer edge. From these relationships, the temperature ratio can be defined as:

$$R = \frac{1 + 0.2 r M_e^2}{1 + 0.2 M_e^2} \quad (8)$$

which is a function of the recovery factor and the local Mach number. The local Mach number can be written

$$M_e = M_e(M_\infty, \delta) \quad (9)$$

where ∞ identifies the free-stream property and δ is the local surface angle of attack.

The local Mach number can be approximated by using tangent cone flow theory, and was used in Equation (8) to give R as a function of M_∞ and δ . Calculations of R were made for several values of M_∞ and δ , and the results were curve fit by Rockwell International. The following equation resulted

$$R(M_\infty, \delta) = a_1 + a_2 \cdot (\sin \delta)^{a_3} \quad (10)$$

where a_1, a_2, a_3 are constants for a particular Mach number. The values of a_1, a_2, a_3 used for this test are:

M_∞	a_1	a_2	a_3
3.0	0.9345	0.1004	2.165
4.0	0.922	0.1004	1.965

Standard matrix techniques, Ref. 3, were used to derive the following relations for δ , as applicable to the model geometry.

$$\delta = \arcsin (\sin \lambda \cos \alpha_s + \cos \lambda \cos \epsilon \sin \alpha_s), \text{ deg} \quad (11)$$

where

$$\epsilon = \text{roll model} + (\theta + 180), \text{ deg; for external tank}$$

$$\epsilon = \text{roll model} + (\psi + 180), \text{ deg; for left SRB}$$

$$\epsilon = \text{roll model} + (180 - \psi), \text{ deg; for right SRB}$$

Additional information would have been required pertaining to the directional cosines at each thermocouple location to calculate δ on the orbiter. This would be necessary since the orbiter model is not symmetrical about the axial centerline. However, this additional information was not available so a modified approach was selected. The equations for calculating δ for the various thermocouples on the orbiter model are shown in Table 3.

The method used to calculate the analytical temperature ratio, R has been applied to all of the tabulated data. The method represents a simplified approach to present a more realistic evaluation of TAW. However, in regions of separated flow or complex interaction, the values calculated for R may no longer apply and should be used with extreme care.

3.4 UNCERTAINTY OF MEASUREMENTS

3.4.1 Test Conditions

The accuracy of the basic measurements (p_o and T_o) was discussed in Section 2.3. Based on repeat calibrations, these errors were found to be

$$\frac{\Delta p_o}{p_o} = 0.002 = 0.2\%, \quad \frac{\Delta T_o}{T_o} = 0.005 = 0.5\%$$

Uncertainties in the basic tunnel parameters p_o and T_o (see Section 2.3) and the two-sigma deviation in Mach number determined from test section flow calibrations were used to estimate uncertainties in the other free-stream properties, using the Taylor series method of propagation, i. e.

$$(\Delta F)^2 = \left(\frac{\partial F}{\partial X_1} \Delta X_1 \right)^2 + \left(\frac{\partial F}{\partial X_2} \Delta X_2 \right)^2 + \left(\frac{\partial F}{\partial X_3} \Delta X_3 \right)^2 \dots + \left(\frac{\partial F}{\partial X_n} \Delta X_n \right)^2 \quad (11)$$

where ΔF is the absolute uncertainty in the dependent parameter $F = F(X_1, X_2, X_3 \dots X_n)$ and X_n is the independent parameter (or basic measurement). ΔX_n is the uncertainty (error) in the independent measurement (or variable).

The computed uncertainties in the tunnel free-stream conditions are summarized in the following table.

<u>Uncertainty, (\pm) percent of actual value</u>				
<u>M_∞</u>	<u>M_∞</u>	<u>P_∞</u>	<u>q_∞</u>	<u>RE/FT</u>
3.0	0.6	2.6	1.4	1.2
4.0	0.4	2.4	1.5	1.2

The uncertainty in model angle of attack (ALPHA-MODEL), as determined from tunnel sector calibration and consideration for possible sting deflections, is estimated to be ± 0.5 deg.

3.4.2 Test Data

Estimated uncertainties in w, b, c in Eq. (2) combined with computed uncertainties for $(dT_w/dt)/(0.95T_o - T_w)^P$ in the Taylor series method of error

propagation gave the following uncertainties in the heat-transfer coefficient for the listed range of values:

<u>H(0.95T₀), Btu</u>	<u>ft²-sec²°R</u>	<u>Uncertainty, percent(±)</u>
	10 ⁻²	9.5
	10 ⁻³	11
	10 ⁻⁴	12

The data were deleted from the results for thermocouples which consistently exceeded the above quoted uncertainties.

4.0 DATA PACKAGE PRESENTATION

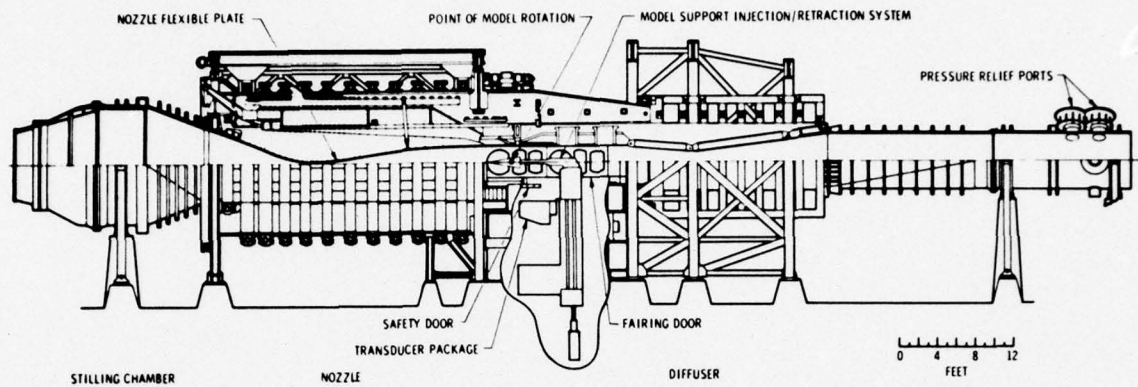
Convective heat-transfer-rate distributions were obtained on a 0.0175-scale model of the Space Shuttle Integrated Model. Typical data tabulations are illustrated in Fig. 5. The final tabulated data were transmitted with this report to NASA-JSC and Rockwell International.

Representative data from the top centerline of the external tank ($\theta = 0$ deg) are presented for a free stream Mach number of 3.01 and 4.02 in Figs. 6 and 7, respectively. These data were obtained with the model in the OTS configuration. The location of the orbiter nose and each SRB nose is located on each figure in terms of the X/L for the external tank. The theoretical data for each Mach number is based on the external tank alone with no protuberances. The theoretical data were derived by using calculations described in Refs. 4 and 5. In general, the data are in good agreement with the theoretical values on the ogive section of the external tank at both Mach numbers. In this region the flow is not disturbed by the other model components and closely approximates the assumptions stated for the theoretical calculations. The trend toward the junction of the nose ogive with the cylindrical body has been consistently observed on the external tank but is not adequately predicted by the theory. The data agreement with the data from a previous test, (IH-72) is generally very good for both Mach numbers. The agreement with theoretical heat-transfer-rates and with previous data is considered as adequate for validation of the basic test results.

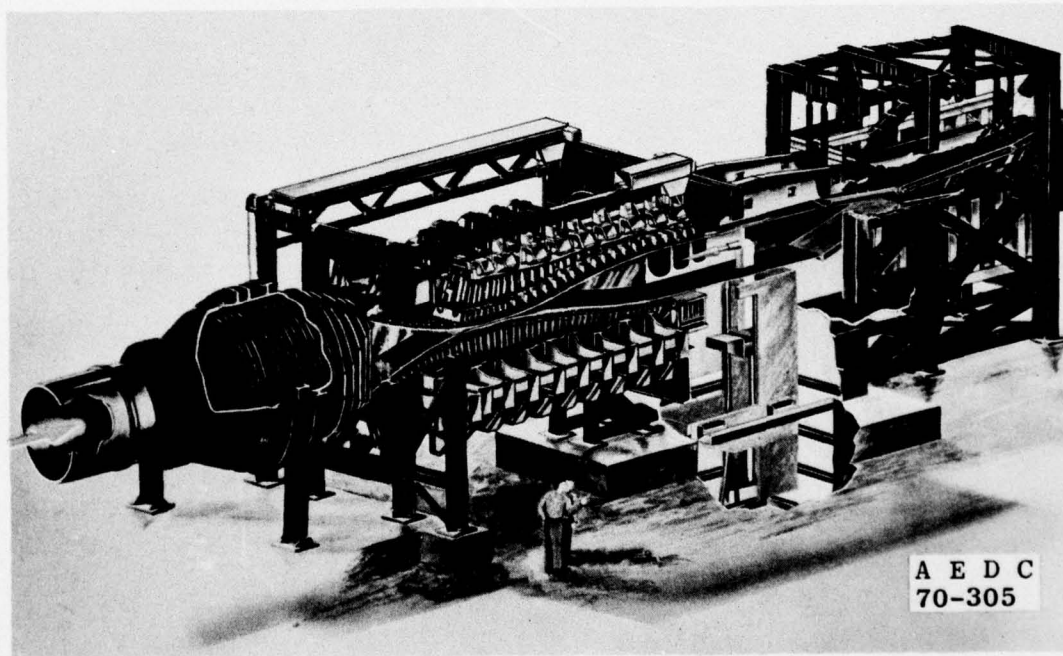
REFERENCES

1. Test Facilities Handbook (Tenth Edition) "von Karman Gas Dynamics Facility," Arnold Engineering Development Center, May 1974.
2. Hilsch, R. "The Use of the Expansion of Gases in a Centerifugal Field as a Cooling Process." The Review of Scientific Instruments, Vol. 18, No. 2, February 1947.
3. Trimmer, L. L. and Clark, E. L. "Transformation of Axes Systems by Matrix Methods and Applications to Wind Tunnel Data Reduction." AEDC-TDR-63-224, October 1963.
4. DeJarnette, Fred R. "Calculation of Inviscid Surface Streamlines on Shuttle-Type Configurations, Part I - Description of Basic Method." NASA CR-111921, August 1971.
5. DeJarnette, Fred R. and Jones, Michael H. "Calculation of Inviscid Surface Streamlines and Heat Transfer on Shuttle Type Configurations, Part 2 - Description of Computer Program." NASA CR-111922, August 1971.

APPENDIX A
ILLUSTRATIONS



a. Tunnel assembly



b. Tunnel test section
Fig. 1 Tunnel A

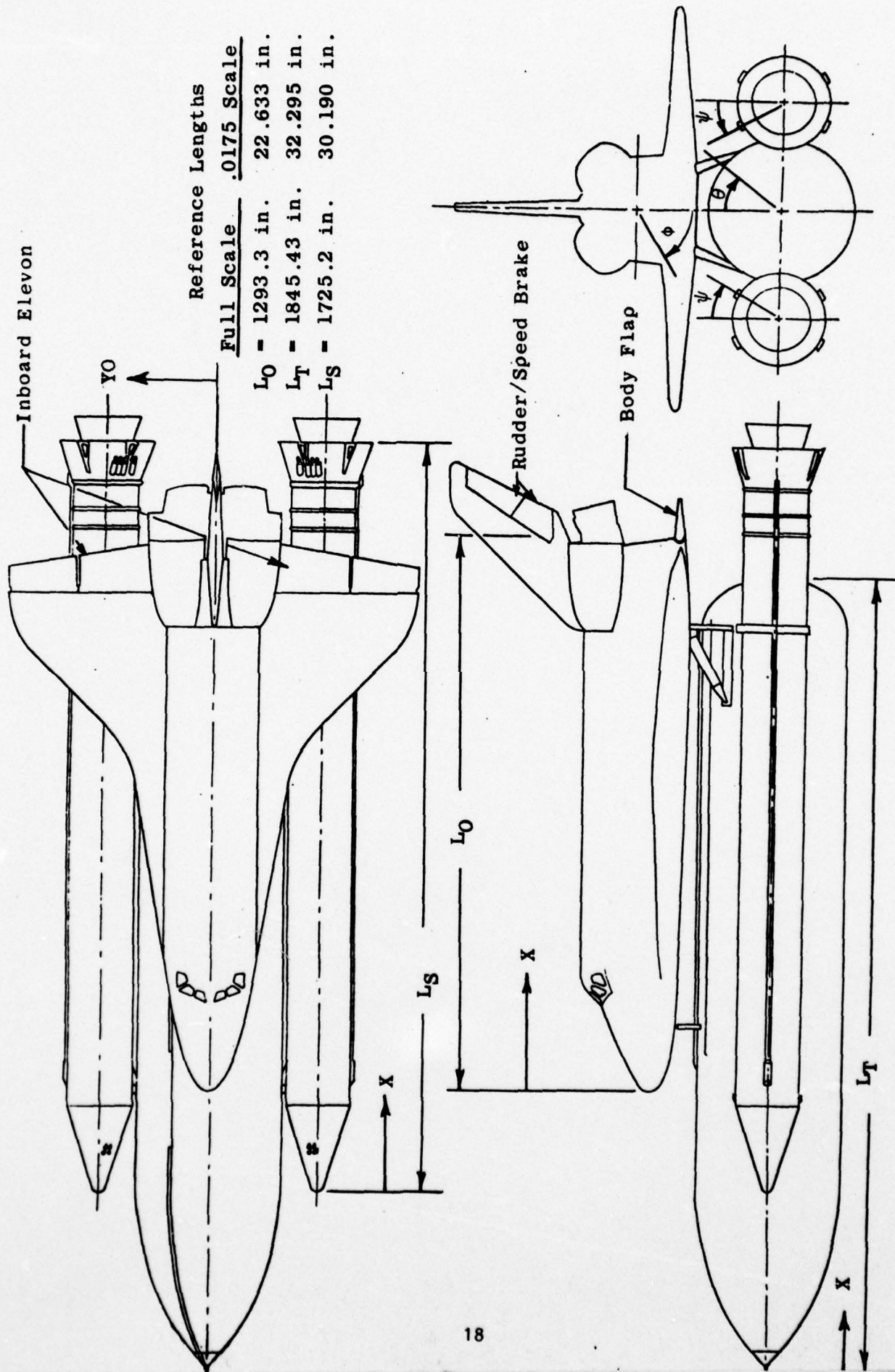


Figure 2. Sketch of the Space Shuttle Integrated Model

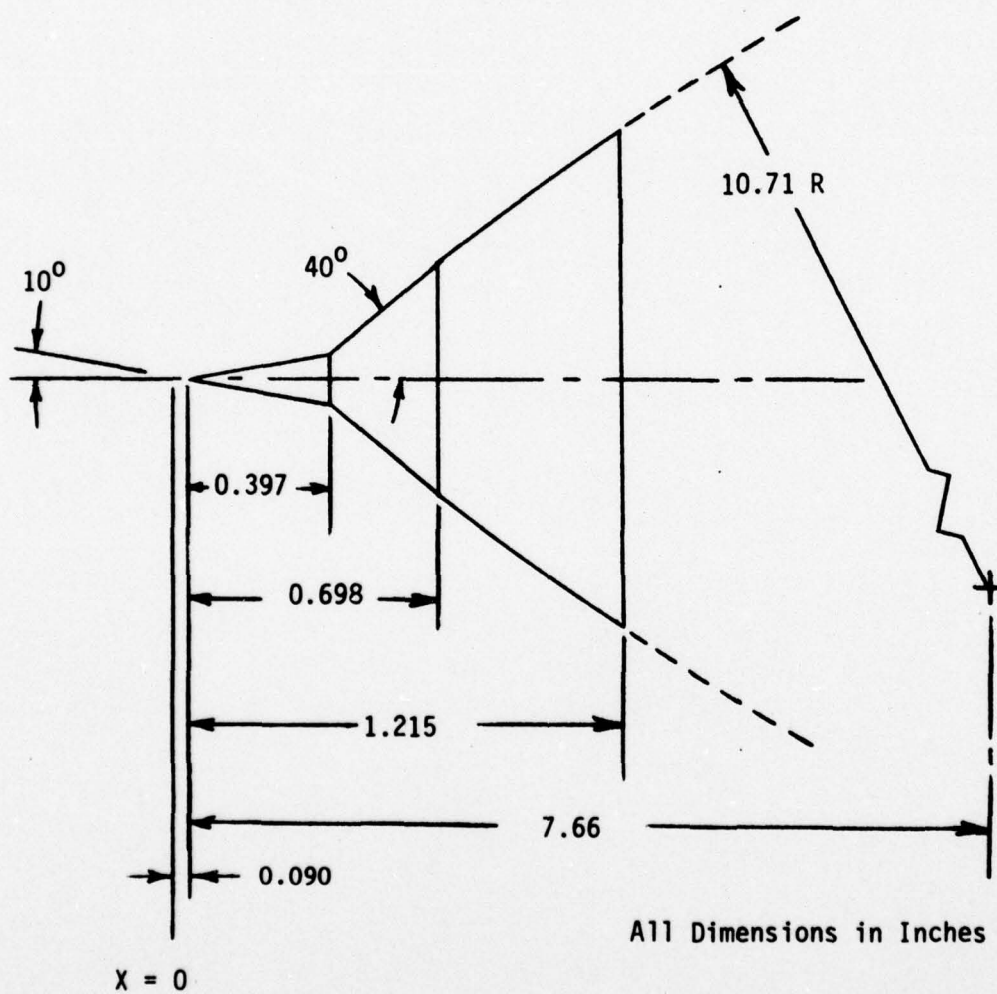


Fig. 3 External Tank Nose Tip Configuration

40-INCH SUPERSONIC TUNNEL A

Scale - 1/5

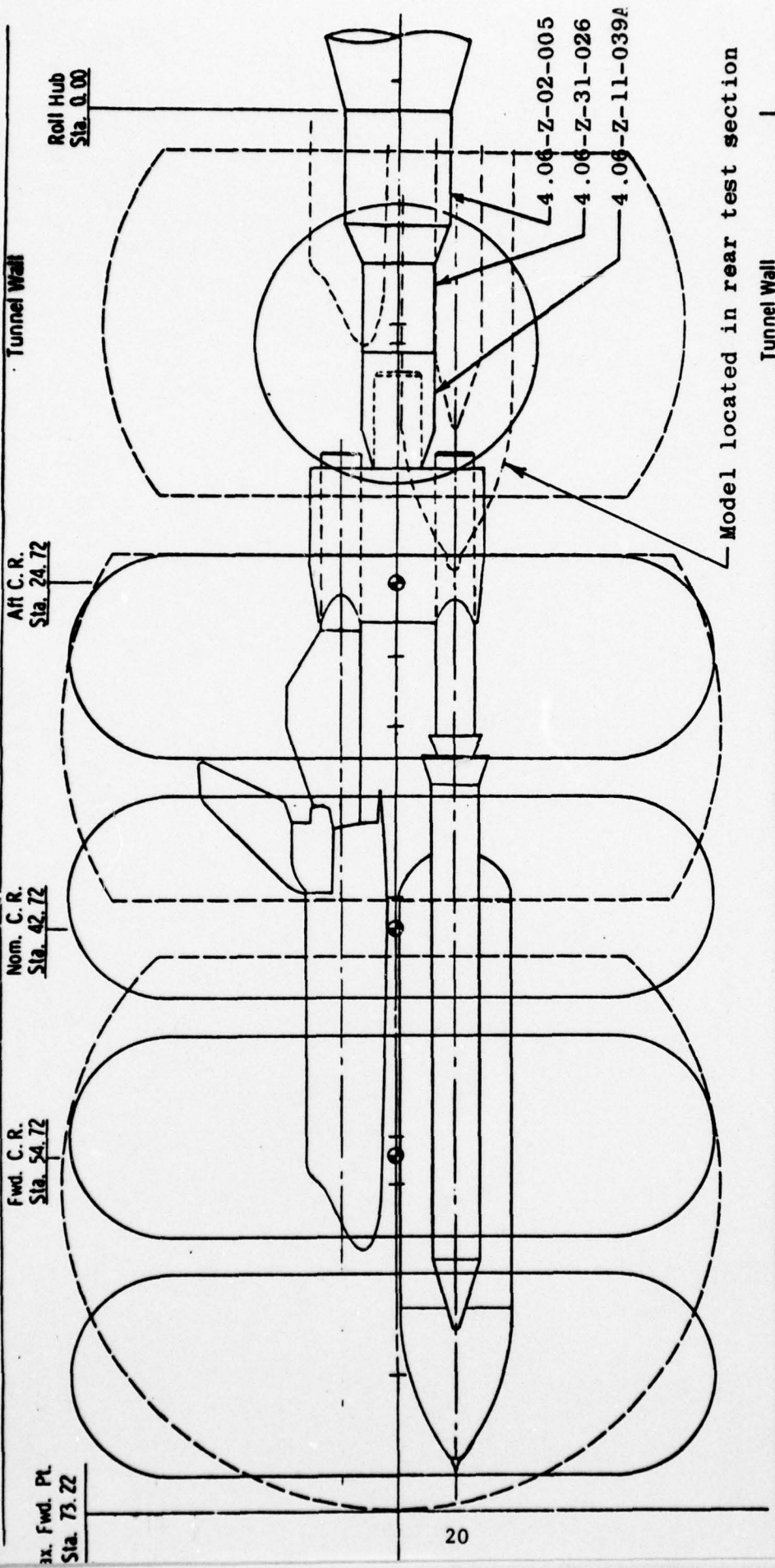
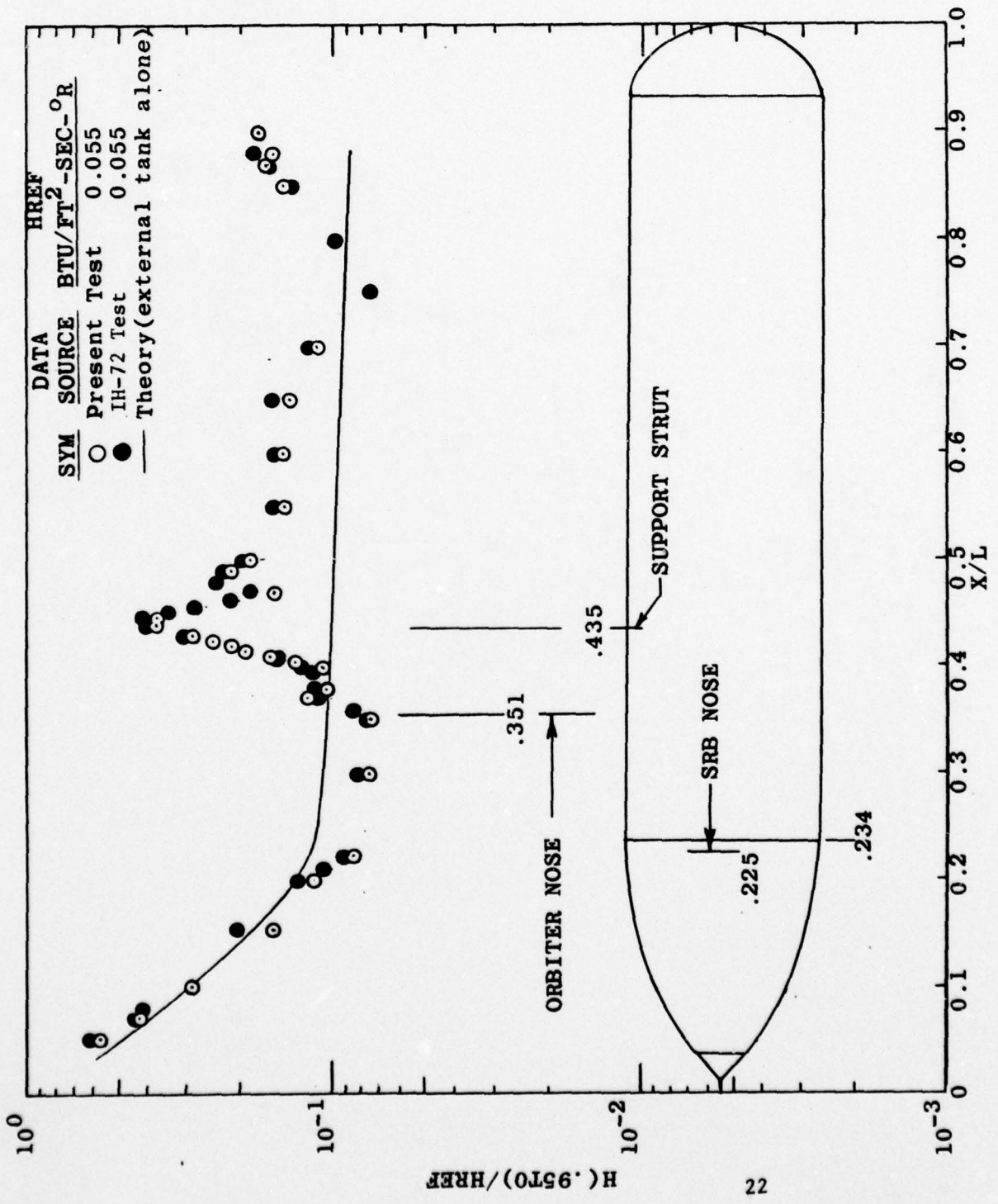


Figure 4. Model Installation in Tunnel A



OTS CONFIGURATION
 THETA = 0 deg

$M_\infty = 3.01$

$\alpha_m = 0$ deg

YAW = 0 deg

RE/FT = 3.8×10^6 , ft⁻¹

Figure 6. Comparison of External Tank Data for the OTS Configuration with Theory and Results from a Previous Test at Mach 3.01

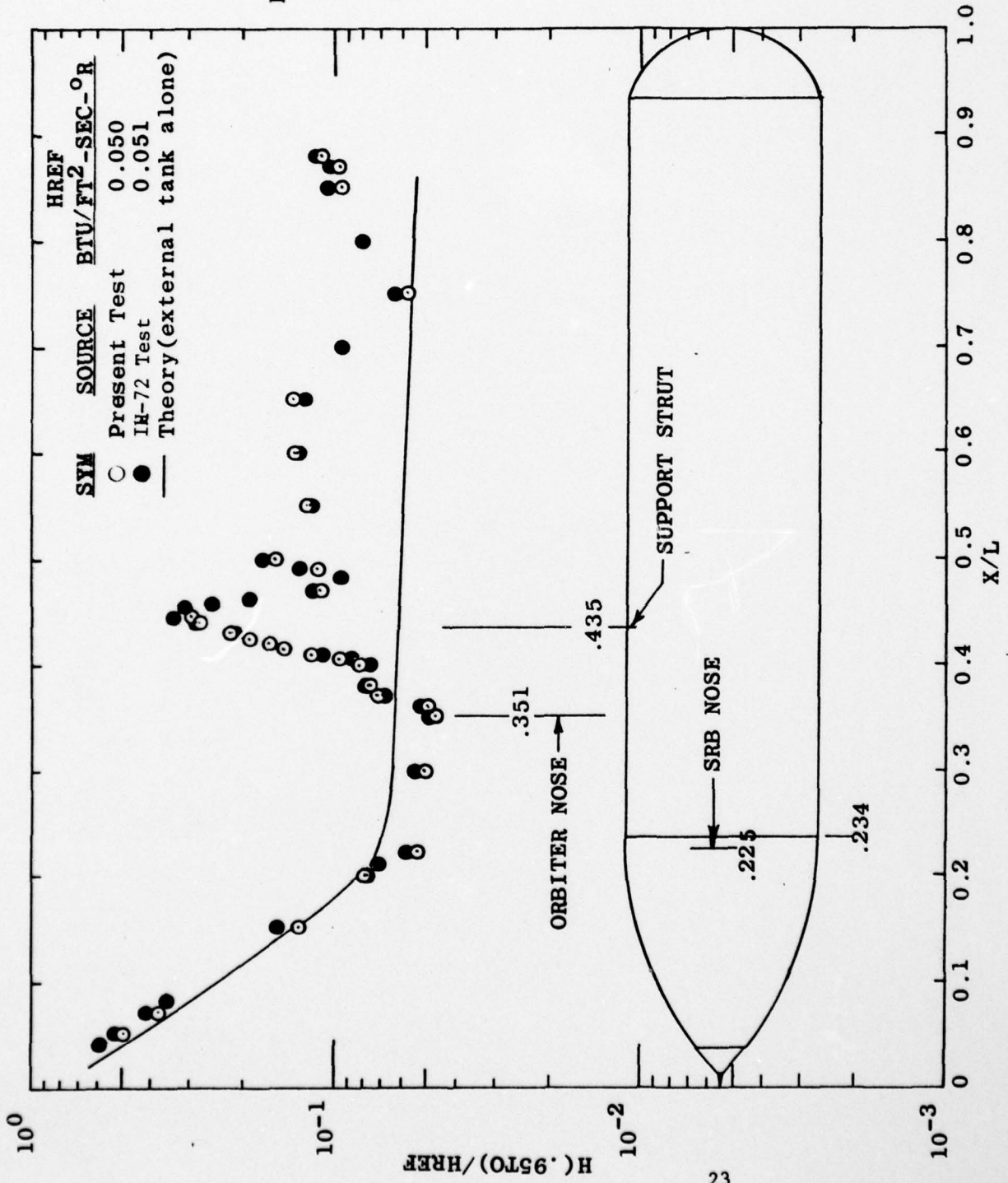


Figure 7. Comparison of External Tank Data for the OTS Configuration with Theory and Results from a Previous Test at Mach 4.02

APPENDIX B

TABLES

TABLE 1. THERMOCOUPLE CONSTANT SETS
EXTERNAL TANK
CONSTANT SET 111

Ch. No.	T/C	X/L	θ
1	615	.38	0
2	616	.385	
3	617	.39	
4	618	.395	
5	619	.40	
6	620	.405	
7	621	.41	
8	622	.415	
9	623	.42	
10	624	.425	
11	625	.43	
12	626	.44	
13	627	.445	
14	628	.45	
15	629	.455	
16	630	.46	
17	631	.47	
18	632	.48	
19	633	.49	
20	634	.50	
21	635	.55	
22	636	.60	
23	637	.65	
24	638	.70	
25	639	.75	
26	640	.80	
27	641	.85	
28	642	.86	
29	643	.87	
30	644	.88	
31	645	.89	
32	646	.90	
33	648	.926	

Ch. No.	T/C	X/L	θ
34	649	.95	0
35	650	.35	11.25
36	651	.36	
37	652	.37	
38	653	.375	
39	654	.38	
40	655	.385	
41	656	.39	
42	657	.395	
43	658	.40	
44	659	.405	
45	660	.41	
46	676	.85	
47	677	.86	
48	678	.87	
49	679	.88	
50	680	.89	
51	681	.90	
52	682	.91	
53	683	.926	
54	684	.95	
55	685	.33	17
56	686	.34	
57	687	.35	
58	688	.36	
59	689	.37	
60	690	.375	
61	691	.50	
62	692	.60	
63	693	.70	
64	694	.80	
65	695	.87	

Ch. No.	T/C	X/L	θ
66	696	.926	17
67	OPEN		
68	OPEN		
69	699	.05	29.8
70	700	.07	
71	701	.10	
72	702	.15	
73	703	.20	
74	704	.30	
75	705	.35	
76	706	.375	
77	707	.50	
78	708	.60	
79	709	.70	
80	710	.80	
81	711	.87	
82	712	.926	
83	OPEN		
84	OPEN		
85	715	.05	37.7
86	716	.07	
87	717	.10	
88	718	.15	
89	719	.20	
90	720	.30	
91	721	.35	
92	722	.375	
93	723	.50	
94	724	.60	
95	725	.70	
96	726	.80	
97	727	.87	

TABLE 1. Continued
EXTERNAL TANK

CONSTANT SET 122

Ch. No.	T/C	X/L	θ
1	728	.926	37.7
2	OPEN		
3	OPEN		
4	2181	.01	180
5	2182	.015	
6	2183	.02	
7	2184	.025	
8	2185	.03	
9	843	.30	292.5
10	844	.33	
11	845	.35	
12	846	.37	
13	847	.40	
14	848	.45	
15	849	.50	
16	850	.55	
17	851	.60	
18	852	.65	
19	853	.70	
20	854	.75	
21	855	.80	
22	856	.90	
23	857	.84	305.4
24	858	.85	
25	859	.86	
26	860	.87	
27	861	.88	
28	862	.89	
29	863	.90	
30	864	.91	
31	865	.926	
32	866	.80	309.3
33	867	.81	

Ch. No.	T/C	X/L	θ
34	868	.82	309.3
35	869	.83	
36	870	.04	315
37	871	.05	
38	872	.06	
39	888	.85	
40	889	.86	
41	890	.87	
42	891	.88	
43	892	.89	
44	893	.90	
45	894	.91	
46	895	.926	
47	896	.95	
48	897	.42	322.3
49	898	.435	
50	899	.45	
51	900	.50	
52	901	.60	
53	902	.70	
54	903	.80	
55	904	.87	
56	905	.42	330.2
57	906	.435	
58	907	.45	
59	908	.50	
60	909	.60	
61	910	.70	
62	911	.80	
63	912	.87	
64	913	.935	
65	914	.945	

Ch. No.	T/C	X/L	θ
66	915	.04	337.5
67	916	.05	
68	917	.06	
69	918	.07	
70	919	.08	
71	920	.10	
72	921	.15	
73	922	.20	
74	923	.42	
75	924	.435	
76	925	.45	
77	926	.85	
78	927	.86	
79	928	.87	
80	929	.88	
81	930	.89	
82	931	.90	
83	932	.91	
84	963	.455	348
85	964	.46	
86	965	.47	
87	966	.48	
88	967	.49	
89	968	.85	
90	969	.86	
91	970	.87	
92	971	.88	
93	972	.89	
94	973	.90	
95	974	.91	
96	975	.926	
97	976	.95	

TABLE 1. Continued
EXTERNAL TANK

CONSTANT SET 133

Ch. No.	T/C	X/L	θ
1	2186	.02	0
2	2187	.025	↓
3	2188	.03	↓
4	985	.04	270
5	986	.05	↓
6	987	.06	↓
7	988	.07	↓
8	989	.08	↓
9	990	.10	↓
10	991	.15	↓
11	992	.20	↓
12	993	.01	39
13	994	.025	↓
14	OPEN		
15	995	.03	39
16	OPEN		
17	OPEN		
18	OPEN		
19	2000	.435	23.07
20	2001	.569	↓
21	2002	.703	↓
22	2003	.836	↓
23	2004	.899	↓
24	OPEN		
25	2005	.476	31.43
26	2006	.511	↓
27	2007	.546	↓
28	2008	.581	↓
29	2009	.616	↓
30	2010	.651	↓
31	OPEN		
32	OPEN		
33	OPEN		

Ch. No.	T/C	X/L	θ
34	2014	.686	31.43
35	2015	.720	↓
36	2016	.756	↓
37	2017	.790	↓
38	2018	.825	↓
39	2019	.860	↓
40	2020	.895	↓
41	2021	.441	326.9
42	2022	.476	↓
43	2023	.511	↓
44	2024	.547	↓
45	2025	.582	↓
46	2026	.617	↓
47	2027	.652	↓
48	2028	.687	↓
49	2029	.723	↓
50	2030	.758	↓
51	2031	.793	↓
52	2032	.828	↓
53	2033	.864	↓
54	2034	.899	↓
55	2035	.934	↓
56	2036	.250	45
57	2037	.300	↓
58	2038	.325	↓
59	2039	.350	↓
60	2040	.375	↓
61	2041	.400	↓
62	2042	.420	↓
63	2043	.425	↓
64	2044	.430	↓
65	2045	.435	↓

Ch. No.	T/C	X/L	θ
66	2046	.44	45
67	2047	.45	↓
68	2048	.47	↓
69	2049	.55	↓
70	2050	.60	↓
71	2051	.65	↓
72	2052	.75	↓
73	2053	.80	↓
74	2054	.83	↓
75	2055	.84	↓
76	2056	.85	↓
77	2057	.86	↓
78	2058	.87	↓
79	2059	.88	↓
80	2060	.89	↓
81	2061	.90	↓
82	2062	.91	↓
83	2063	.926	↓
84	2064	.935	↓
85	2065	.945	↓
86	2066	.25	36.32
87	2067	.30	↓
88	2068	.325	↓
89	2069	.35	↓
90	2070	.375	↓
91	2071	.40	↓
92			
93			
94			
95			
96			
97			

TABLE 1. Continued
EXTERNAL TANK

CONSTANT SET 211

Ch. No.	T/C	X/L	θ
1	2089	.937	352.2
2	2088	↓	289.4
3	2087	↓	250.6
4	2090	.355	29.8
5	2091	.360	↓
6	2092	.365	↓
7	2093	.370	↓
8	2094	.355	23.08
9	2095	.360	↓
10	2096	.365	↓
11	2097	.370	↓
12	2098	.355	20.98
13	2099	.360	↓
14	2100	.365	↓
15	2101	.370	↓
16	2102	.355	17.0
17	OPEN		
18	2104	.400	330.2
19	2105	.405	↓
20	2106	.410	↓
21	2107	.400	326.8
22	2108	.405	↓
23	2109	.405	324.5
24	2110	.410	↓
25	2111	.410	315
26	2112	.835	309.3
27	2113	.820	305.4
28	2114	.830	↓
29	2115	.835	↓
30	2116	.820	301.5
31	2117	.830	↓
32	2118	.835	↓
33	2119	.840	↓

Ch. No.	T/C	X/L	θ
34	2120	.85	301.5
35	2121	.86	↓
36	2122	.87	↓
37	2123	.88	↓
38	2124	.89	↓
39	2125	.90	↓
40	OPEN		
41	2127	.925	301.5
42	2128	.935	↓
43	2129	.82	292
44	2130	.83	↓
45	2131	.84	↓
46	2132	.85	↓
47	2133	.86	↓
48	2134	.87	↓
49	2135	.88	↓
50	2136	.89	↓
51	2137	.91	↓
52	2138	.926	↓
53	2139	.93	↓
54	2140	.926	299.4
55	2141	↓	270
56	2142	↓	258
57	2143	↓	250.6
58	2144	↓	247.5
59	2145	.93	289.4
60	2146	↓	270
61	2147	↓	258
62	2148	↓	250.6
63	2149	↓	247.5
64	2150	.935	270
65	2151	↓	258

Ch. No.	T/C	X/L	θ
66	2152	.926	33.75
67	2153	↓	31.75
68	2154	↓	23.07
69	OPEN		
70	OPEN		
71	OPEN		
72	2158	.926	355.2
73	OPEN		
74	2160	.926	345.2
75	2161	↓	335
76	2162	↓	330.2
77	2163	↓	326.9
78	2164	↓	324.5
79	OPEN		
80	2166	.441	31.43
81	2167	.425	337.5
82	2168	↓	345.6
83	2169	↓	354
84	2170	↓	5.63
85	2171	↓	17
86	2172	.430	337.5
87	2173	↓	345.6
88	2174	↓	354
89	2175	↓	5.63
90	2176	↓	17
91	600	.04	0
92	601	.05	↓
93	602	.06	↓
94	603	.07	↓
95	604	.08	↓
96	605	.10	↓
97	606	.15	↓

TABLE 1. Continued
EXTERNAL TANK AND RIGHT SRB
CONSTANT SET 222

Ch. No.	T/C	X/L	θ/ψ^*
1	607	.20	0
2	608	.21	↓
3	609	.22	↓
4	610	.30	↓
5	611	.35	↓
6	612	.36	↓
7	613	.37	↓
8	614	.375	↓
9	1478	.937	263
10	1500	.953	0
11	1501	.965	↓
12	1502	.975	↓
13	1503	.985	↓
14	1504	.995	↓
15	1505	.953	24
16	1506	.967	23
17	1507	.980	22
18	1508	.994	21
19	1509	.954	30
20	1510	.953	36
21	1511	.967	323
22	1512	.980	322
23	1513	.994	321
24	1514	.953	315
25	1515	.953	306
26	1516	.967	308
27	1517	.980	↓
28	1518	.994	↓
29	1519	.953	234
30	1520	.965	230
31	1521	.975	↓
32	1522	.985	↓
33	1523	.953	225

Ch. No.	T/C	X/L	ψ
34	1524	.967	225
35	1525	.953	216
36	1526	.965	217
37	1527	.975	218
38	1528	.985	219
39	1529	.995	220
40	1530	.954	210
41	1531	.953	156
42	1532	.967	157
43	1533	.980	158
44	1534	.994	159
45	1535	.953	204
46	1536	.967	203
47	1537	.980	202
48	1538	.994	201
49	1539	.954	210
50	1540	.953	216
51	1541	.967	217
52	1542	.980	218
53	1543	.994	219
54	1544	.953	320
55	1545	.965	↓
56	1546	.985	↓
57	1547	.975	322.5
58	1548	.985	↓
59	1549	.954	330
60	1550	.995	340
61	1551	.985	345
62	1552	.995	↓
63	1553	.985	350
64	1554	.995	↓
65	1555	.953	355

Ch. No.	T/C	X/L	ψ
66	1556	.985	355
67	1557	.964	330.7
68	1558	.978	↓
69	1559	.982	320
70	1560	.954	324
71	1561	.975	↓
72	1562	.954	336
73	1563	.982	334
74	1564	.975	336
75	1565	.982	340
76	1566	.954	342
77	1567	.964	↓
78	1568	.975	↓
79	1569	.982	350
80	1570	.975	353
81	OPEN		
82	OPEN		
83	OPEN		
84	1574	.971	11
85	1575	.978	11
86			
87			
88			
89			
90			
91			
92			
93			
94			
95			
96			
97			

* θ Applies through Channel 8, ψ starts with Channel 9

TABLE 1. Continued
ORBITER

CONSTANT SET 233

Ch. No.	T/C	X/L	ϕ
1	OPEN		
2	227	.60	157.5
3	228	.65	↓
4	229	.70	
5	230	.75	↓
6	234	.40	135
7	238	.60	↓
8	239	.65	
9	240	.70	
10	241	.75	↓
11	242	.80	
12	392	.60	114
13	393	.65	
14	394	.70	
15	395	.75	
16	OPEN		
17	7	.05	0
18	8	.06	↓
19	9	.07	
20	10	.08	
21	11	.09	
22	12	.10	↓
23	207	.10	20
24	208	.10	24.5
25	13	.12	0
26	14	.13	↓
27	15	.14	
28	16	.15	
29	17	.16	
30	18	.17	
31	19	.18	↓
32	299	.843	
33	300	.843	

Ch. No.	T/C	X/L	ϕ
34	301	.843	
35	302	.862	
36	OPEN		
37	304	.862	
38	305	↓	
39	306	↓	
40	308	.881	
41	309	↓	
42	310	↓	
43	311	↓	
44	OPEN		
45	312	.881	
46	315	.920	
47	316	↓	
48	317	↓	
49	318	↓	
50	319	↓	
51	320	.939	
52	321	↓	
53	322	↓	
54	323	↓	
55	325	↓	
56	327	.978	
57	328	↓	
58	329	↓	
59	330	↓	
60	331	↓	
61	332	.997	
62	333	↓	
63	334	↓	
64	335	↓	
65	337	1.01	

Ch. No.	T/C	X/L	ϕ
66	338	1.01	
67	339	↓	
68	OPEN		
69	183	.45	180
70	185	.55	↓
71	187	.65	↓
72	OPEN		
73	190	.80	180
74	506	.868	--
75	509	.847	
76	515	.839	
77	521	.858	
78	522	.870	
79	523	.837	
80	527	.861	
81	534	.830	
82	538	.868	
83	542	.833	
84	20	.19	0
85	21	.20	↓
86	23	.25	
87	24	.30	
88	25	.35	
89	26	.40	
90	27	.45	
91	28	.50	
92	29	.55	
93	OPEN		
94	32	.70	
95	33	.75	
96	36	.90	↓
97			

TABLE 1. Continued
LEFT SRB

CONSTANT SET 311

Ch. No.	T/C	X/L	ψ
1	1000	.115	0
2	1001	.20	
3	1002	.225	
4	1003	.25	
5	1004	.30	
6	1005	.40	
7	1006	.50	
8	1007	.55	
9	1008	.60	
10	1009	.65	
11	1010	.70	
12	1011	.75	
13	1012	.80	
14	1013	.875	
15	1014	.925	
16	1015	.939	
17	1016	.953	355
18	1017	.967	
19	1018	.980	
20	1019	.994	
21	1020	.115	45
22	1021	.143	
23	1022	.171	
24	1023	.20	
25	1024	.30	
26	1025	.40	
27	1026	.50	
28	1027	.55	
29	1028	.60	
30	1029	.65	
31	1030	.70	
32	1031	.80	
33	1032	.875	

Ch. No.	T/C	X/L	ψ
34	1033	.925	45
35	1034	.953	50
36	1035	.967	
37	1036	.980	
38	1037	.994	
39	1038	0	90
40	1039	.002	
41	1040	.008	
42	1041	.050	
43	1042	.10	
44	1043	.12	
45	1044	.127	
46	1045	.134	
47	1046	.173	
48	1047	.180	
49	1048	.186	
50	1049	.193	
51	1050	.20	
52	1051	.25	
53	1052	.30	
54	1053	.40	
55	1054	.50	
56	1055	.60	
57	1056	.70	
58	1057	.75	
59	1058	.80	
60	1059	.875	
61	1060	.925	
62	1061	.953	
63	1062	.967	
64	1063	.980	
65	1064	.994	

Ch. No.	T/C	X/L	ψ
66	1065	.115	135
67	1066	.143	
68	1067	.171	
69	1068	.20	
70	1069	.30	
71	1070	.50	
72	1071	.60	
73	1072	.70	
74	1073	.80	
75	1074	.953	
76	1124	.177	315
77	1125	.20	
78	1126	.30	
79	1127	.50	
80	1128	.60	
81	1129	.70	
82	1130	.80	
83	1131	.875	
84	1132	.925	
85	1133	.953	
86	1134	.967	
87	1135	.980	
88	1136	.994	
89	1200	.043	65
90	1201	.05	
91	1202	.057	
92	1203	.063	
93	1204	.090	
94	1205	.10	
95	1206	.05	35
96	1207	.09	
97	1208	.10	

TABLE 1. Continued
LEFT AND RIGHT SRB *

CONSTANT SET 322

Ch. No.	T/C	X/L	ψ	Ch. No.	T/C	X/L	ψ	Ch. No.	T/C	X/L	ψ
1	1209	.05	5	34	1244	.75	225	66	1276	.953	198
2	1210	.09	↓	35	1245	↓	315	67	1277	↓	238
3	1211	.10	↓	36	1246	↓	135	68	1278	.967	302
4	1212	.043	335	37	1247	.771	180	69	1279	↓	342
5	1213	.05	↓	38	1248	↓	225	70	1280	↓	198
6	1214	.057	↓	39	OPEN			71	1281	↓	238
7	1215	.063	↓	40	1250	.771	315	72	1282	.98	302
8	1216	.090	↓	41	1251	↓	0	73	1283	↓	342
9	1217	.10	↓	42	1252	↓	135	74	1284	↓	198
10	1220	.965	4.38	43	1253	.932	180	75	1285	↓	238
11	1221	.975	↓	44	1254	↓	225	76	1286	.994	302
12	1222	.985	↓	45	OPEN			77	1287	↓	342
13	1223	.995	↓	46	1256	.932	315	78	1288	↓	198
14	1224	.965	20	47	1257	↓	0	79	1289	↓	238
15	1225	.975	↓	48	1258	↓	45	80	1290	.12	76
16	1226	.985	↓	49	1259	↓	135	81	1291	.127	↓
17	1227	.995	↓	50	1260	.939	180	82	1292	.134	↓
18	1228	.965	40	51	1261	↓	225	83	1293	.173	↓
19	1229	.975	↓	52	OPEN			84	1300	.025	180
20	1230	.985	↓	53	1263	.939	315	85	1302	.075	↓
21	1231	.995	↓	54	1264	↓	45	86	1305	.025	270
22	1232	.724	0	55	1265	↓	135	87	1307	.075	↓
23	1233	.724	225	56	1266	.953	138	88	1311	.025	0
24	OPEN			57	1267	↓	162	89	1313	.075	5
25	1235	.724	315	58	1268	.967	138	90	1314	.110	5
26	1236	↓	330	59	1269	↓	162	91	1316	.075	20
27	1237	↓	135	60	1270	.98	138	92	1317	.090	20
28	1238	.74	180	61	1271	↓	162	93	1318	.100	↓
29	1239	↓	225	62	1272	.994	138	94	1319	.110	↓
30	OPEN			63	1273	↓	162	95	1321	.075	35
31	1241	.74	315	64	1274	.953	302	96	1322	.110	↓
32	1242	↓	0	65	1275	↓	342	97	1323	.110	65
33	1243	↓	135								

* Thermocouples on the LEFT SRB (Channels 1-83), RIGHT SRB (Channels 84-97)

TABLE 1. Continued *
LEFT AND RIGHT SRB *

CONSTANT SET 333

Ch. No.	T/C	X/L	ψ	Ch. No.	T/C	X/L	ψ	Ch. No.	T/C	X/L	ψ
1	1324	.10	76	34	1383	.74	67.5	66	1418	.750	112.5
2	1326	.025	90	35	1384	.75	↓	67	1420	.925	↓
3	1328	.06	↓	36	1386	.141	76	68	1421	.932	↓
4	1329	.075	↓	37	1387	.148	↓	69	1422	.939	↓
5	1330	.10	104	38	1388	.155	↓	70	1423	.40	135
6	1332	.025	135	39	1389	.162	↓	71	1425	.98	225
7	1334	.075	↓	40	1390	.25	↓	72	1426	.994	↓
8	1335	.10	↓	41	1393	.74	90	73	1430	.953	4.25
9	1336	.136	263	42	1394	.765	↓	74	1431	↓	15.6
10	1344	.939	↓	43	1395	.771	↓	75	1432	↓	20
11	1345	.115	270	44	1396	.815	↓	76	1433	↓	24.4
12	1346	.136	277	45	1397	.837	↓	77	1434	↓	35.6
13	1347	.30	↓	46	1398	.884	↓	78	1435	↓	40
14	1348	.75	↓	47	1399	.894	↓	79	1436	↓	77.5
15	1349	.815	↓	48	1400	.907	↓	80	1437	.967	↓
16	1350	.837	↓	49	1401	.917	↓	81	1438	.98	↓
17	1351	.884	↓	50	1402	.932	↓	82	1439	.994	↓
18	1352	.894	↓	51	1403	.939	↓	83	1440	.953	112.5
19	1354	.939	↓	52	1404	.120	104	84	1441	.967	↓
20	1355	.74	337.5	53	1405	.127	↓	85	1442	.98	↓
21	1356	.75	↓	54	1406	.134	↓	86	1443	.994	↓
22	1362	.765	0	55	1407	.141	↓	87	1444	FWD	SEP
23	1363	.815	↓	56	1408	.148	↓	88	1445	MOTORS	↓
24	1364	.837	↓	57	1409	.155	↓	89	1446	↓	↓
25	1365	.884	↓	58	1410	.162	↓	90	1447	↓	↓
26	1366	.907	↓	59	1411	.173	↓	91	1448	↓	↓
27	1368	.74	22.5	60	1412	.180	↓	92	1294	.18	76
28	1369	.75	↓	61	1413	.186	↓	93	1295	.186	↓
29	1372	.925	↓	62	1414	.193	↓	94	1296	.193	↓
30	1373	.932	↓	63	1415	.200	↓	95	1297	.20	↓
31	1374	.939	↓	64	1416	.250	↓	96			
32	1375	.74	45	65	1417	.740	112.5	97			
33	1376	.75	↓								

* Thermocouples on the RIGHT SRB (Channels 1-91), LEFT SRB (Channels 92-95)

TABLE 1. Continued
RIGHT SRB

CONSTANT SET 411

Ch. No.	T/C	X/L	ψ
1	1449	FWD. SEP. MOTORS	
2	1450		
3	1451		
4	1452		
5	1453		
6	1454		
7	1455		
8	1456		
9	1457		
10	1458		
11	1459		
12	1460		
13	1461		
14	1462		
15	1463	.2	277
16	1464	.4	
17	1465	.5	
18	1466	.6	
19	1467	.7	
20	1468	.9	
21	1469	.921	
22	1470	.928	
23	1471	.937	
24	1477	.928	263
25	1479		90
26	1480		
27	1481		
28	1482		
29	1483		
30	1484		95
31	1485		
32	1486		
33	1487		

Ch. No.	T/C	X/L	ψ
34	1488		95
35	1489		112
36	1490		
37	1491		
38	1492		
39	1493		
40	1494		140
41	1495		
42	1496		
43	1497		
44	1498		
45	1499		150
46	1298	.008	180
47	1299	.015	
48	1301	.05	
49	1303	.10	
50	1304	.008	270
51	1306	.05	
52	1308	.10	
53	1309	.11	335
54	1310	.008	0
55	1325	.015	90
56	1327	.04	
57	1331	.008	135
58	1333	.05	
59	1337	.30	263
60	1338	.75	
61	1339	.815	
62	1340	.837	
63	1341	.884	
64	1342	.894	
65	1343	.907	

Ch. No.	T/C	X/L	ψ
66	1353	.907	277
67	1357	.765	337.5
68	1358	.771	
69	1359	.925	
70	1360	.932	
71	1361	.939	
72	1367	.724	22.5
73	1370	.765	
74	1371	.771	
75	1377	.765	45
76	1378	.771	
77	1379	.815	
78	1380	.837	
79	1381	.884	
80	1382	.907	
81	1385	.771	67.5
82	1391	.55	90
83	1392	.65	
84	1419	.771	112.5
85	1424	.925	135
86	1472	.2	263
87	1473	.4	
88	1474	.5	
89	1475	.6	
90	1476	.7	
91			
92			
93			
94			
95			
96			
97			

TABLE 1. Continued
EXTERNAL TANK

CONSTANT SET 511

Ch. No.	T/C	X/L	θ
1	2089	.937	352.2
2	2088	↓	289.4
3	2087	↓	250.6
4	2090	.355	29.8
5	2091	.360	↓
6	2092	.365	↓
7	2093	.370	↓
8	2094	.355	23.08
9	2095	.36	↓
10	2096	.365	↓
11	2097	.37	↓
12	2098	.355	20.98
13	2099	.36	↓
14	2100	.365	↓
15	2101	.37	↓
16	2102	.355	17
17	OPEN		
18	2104	.40	330.2
19	2105	.405	↓
20	2106	.41	↓
21	2107	.40	326.8
22	2108	.405	↓
23	2109	.405	324.5
24	2110	.41	↓
25	2111	.41	315
26	2112	.835	309.3
27	2113	.820	305.4
28	2114	.830	↓
29	2115	.835	↓
30	2116	.820	301.5
31	2117	.830	↓
32	2118	.835	↓
33	2119	.840	↓

Ch. No.	T/C	X/L	θ
34	2120	.85	301.5
35	2121	.86	↓
36	2122	.87	↓
37	2123	.88	↓
38	2124	.89	↓
39	2125	.90	↓
40	OPEN		
41	2127	.925	301.5
42	2128	.935	↓
43	2129	.82	292
44	2130	.83	↓
45	2131	.84	↓
46	2132	.85	↓
47	2133	.86	↓
48	2134	.87	↓
49	2135	.88	↓
50	2136	.89	↓
51	2137	.91	↓
52	2138	.926	↓
53	2139	.930	↓
54	2140	.926	299.4
55	2141	↓	270
56	2142	↓	258
57	2143	↓	250.6
58	2144	↓	247.5
59	2145	.93	289.4
60	2146	↓	270
61	2147	↓	258
62	2148	↓	250.6
63	2149	↓	247.5
64	2150	.935	270
65	2151	↓	258

Ch. No.	T/C	X/L	θ
66	2152	.926	33.75
67	2153	↓	31.75
68	2154	↓	23.07
69	OPEN		
70	OPEN		
71	OPEN		
72	2158	.926	355.2
73	OPEN		
74	2160	.926	345.2
75	2161	↓	335
76	2162	↓	330.2
77	2163	↓	326.9
78	2164	↓	324.5
79	OPEN		
80	2166	.441	31.43
81	2167	.425	337.5
82	2168	↓	345.6
83	2169	↓	354
84	2170	↓	5.63
85	2171	↓	17
86	2172	.430	337.5
87	2173	↓	345.5
88	2174	↓	354
89	2175	↓	5.63
90	2176	↓	17
91	661	.415	11.25
92	662	.42	↓
93	663	.425	↓
94	664	.43	↓
95	665	.44	↓
96	666	.45	↓
97	667	.455	↓

TABLE 1. Concluded
EXTERNAL TANK

CONSTANT SET 522

Ch. No.	T/C	X/L	θ
1	668	.46	11.25
2	669	.47	↓
3	670	.48	↓
4	671	.49	↓
5	672	.50	↓
6	673	.60	↓
7	674	.70	↓
8	675	.80	↓
9	812	.40	258
10	813	.23	270
11	814	.24	↓
12	815	.25	↓
13	816	.27	↓
14	817	.29	↓
15	818	.30	↓
16	819	.31	↓
17	820	.32	↓
18	821	.325	↓
19	822	.33	↓
20	823	.335	↓
21	824	.34	↓
22	825	.345	↓
23	826	.35	↓
24	828	.36	↓
25	829	.365	↓
26	830	.37	↓
27	831	.375	↓
28	832	.38	↓
29	833	.39	↓
30	834	.40	↓
31	835	.50	↓
32	836	.60	↓
33	837	.70	↓

Ch. No.	T/C	X/L	θ
34	838	.80	270
35	839	.90	↓
36	840	.23	292.5
37	841	.25	↓
38	842	.27	↓
39	873	.07	315
40	874	.08	↓
41	875	.10	↓
42	876	.15	↓
43	877	.20	↓
44	878	.35	↓
45	879	.40	↓
46	880	.50	↓
47	881	.55	↓
48	882	.60	↓
49	883	.65	↓
50	884	.70	↓
51	885	.75	↓
52	886	.80	↓
53	887	.84	↓
54	933	.926	337.5
55	934	.415	343.1
56	935	.42	↓
57	936	.425	↓
58	937	.43	↓
59	938	.44	↓
60	939	.445	↓
61	940	.45	↓
62	941	.50	↓
63	942	.60	↓
64	943	.70	↓
65	944	.80	↓

Ch. No.	T/C	X/L	θ
66	945	.35	348
67	946	.36	↓
68	947	.37	↓
69	948	.375	↓
70	949	.38	↓
71	950	.385	↓
72	951	.39	↓
73	952	.395	↓
74	953	.40	↓
75	954	.405	↓
76	955	.41	↓
77	956	.415	↓
78	957	.42	↓
79	958	.425	↓
80	959	.43	↓
81	960	.44	↓
82	961	.445	↓
83	962	.45	↓
84	2072	.42	36.32
85	2073	.425	↓
86	2074	.43	↓
87	2075	.435	↓
88	2076	.45	↓
89	2077	.60	↓
90	2078	.65	↓
91	2079	.25	33.75
92	2080	.30	↓
93	2081	.375	↓
94	2082	.40	↓
95	2083	.43	↓
96	2084	.45	↓
97	2085	.60	↓

TABLE 2. TEST DATA SUMMARY

CONFIGURATION	MACH NUMBER	α_m , deg	β , deg	DATA GROUP NUMBERS																		
				CONSTANT SET																		
				111	122	133	211	222	233	311	322	333	411	111	122	133	211	222	233	311	322	333
OTS	3.01	0	0	25	230	28	3	220	5													
			3	29	231	32	9			11												
			-3	33	232	35	12			13												
			5							224												
			-5							225												
			0							226												
	4.02		5	5					227													
			-5						228													
			0						221													
			5						222													
			-5						223													
			0	47	48	49	84	85	86													
			3	50	51	52	87	88	89	90	168	169	170	208								
			-3					96			171	172	173	209								
			4.5	53	54	55	90			91												
			-4.5	56	57	58	92			93												
			5					94														
			-5					95														
				7.5	59	60	61	97	98	99	174	175	176	210								
				-7.5	63	64	65	100	101	102	177	178	179	211								
				9					103	104												
				-9					105													

Table 2. Continued

CONFIGURATION	MACH NUMBER	α_m , deg	β , deg	DATA GROUP NUMBERS																			
				CONSTANT SET																			
				111	122	133	511	522															
OT	3.01	0	0	234	235	236	368	369															
			3	262	263	264	387	388															
			-3	265	266	267	389	390															
			5	237	238	239	370	371															
			-5	240	241	242	372	373															
			5	243	244	245	374	375															
				268																			
				399	400	401	391	392															
				402			393	394															
				246	247	248	376	377															
				249	250	251	378	379															
				-5	0	253	254	255	381	382													
					3				395	396													
					-3				397	398													
					5	256	257	258	383	384													
			-5	259	260	261	385	386															

Table 2. Concluded

CONFIGURATION	MACH NUMBER	α_m , deg	β , deg	DATA GROUP NUMBERS																	
				111	122	133	511	522	CONSTANT SET												
OT	4.02	0	0	270	271	272	323	324													
			3					364	365												
			-3					366	367												
			5	✓	273	274	275	325	326												
			-5		276	277	278	327	328												
			0	5	279	280	281	329	330												
			3		282	283	284	331	332												
			-3		285	286	287	333	334												
			5		288	289	290	336	337												
			-5	✓	291	292	293	338	341												
			0	-5	295	299	300	342	343												
			3		301	302	303	344	345												
			-3		314	315	316	346	347												
			5		317	318	319	348	349												
			-5	✓	320	321	322	350	353												
	0	-10	304	305	306	354	355														
	3					360	361														
	-3					362	363														
	5		307	308	309	356	357														
	-5	✓	310	311	312	358	359														

Table 3. Equations for Calculating Local Surface Angle of Attack on the Orbiter Model

Orbiter Thermocouple Numbers	Equation for Calculating δ
1 - 168 501 - 548	$\delta = \lambda + \alpha_m$
169 - 201 231 - 280	$\delta = \lambda - \alpha_m$
202 - 230 281 - 292 340 - 396	$\delta = \lambda + \text{Yaw}$
293 - 339	$\delta = \lambda$